X-Ray Analysis of α-, β-, and γ-Phase Ag–Hg Alloy Films Produced on Polymer Substrates by Casting Polyacrylamide–$AgNO_3$ Aqueous Solution in Hg Atmosphere

JIUNN YIH LEE, KIYOTO OHTSUKA,* HIDEO TAKEZOE, ATSUO FUKUDA, and EIICHI KUZE, *Department of Textile and Polymeric Materials, Tokyo Institute of Technology O-okayama, Meguro-ku, Tokyo 152, Japan,* and HIROSHI IWANAGA, *Faculty of Liberal Arts, Nagasaki University Bunkyo-machi, Nagasaki 852, Japan*

Synopsis

It is reported that, by dropping Hg metal on the wet α-phase Ag–Hg alloy film formed on the cast polyacrylamide–$AgNO_3$ aqueous solution, the α phase of fcc structure can be converted into other phases that contain more Hg. The X-ray analysis of these phases reveals that they are the β phase of hexagonal structure and the γ phase of bcc structure. It is also shown that the lattice constant of the α phase can be controlled to some extent by pH of the aqueous solution of PAAm from which the alloy film is formed.

INTRODUCTION

It is known that needlelike crystals of Ag–Hg alloy are formed by adding Hg metal to $AgNO_3$ aqueous solution.[1] All the phases, α, β, and γ, shown in Table I are produced by this method. In our previous article,[2] we reported that Ag–Hg alloy films can be formed on polyacrylamide (PAAm) surfaces by leaving cast PAAm–$AgNO_3$ aqueous solution in Hg-saturated atmosphere. The film formation sensitively depends on polymers used; only the combination of PAAm and $AgNO_3$ has an ability to produce the alloy films. Moreover, the films obtained are apparently manifold, depending on pH of the starting aqueous solution. In spite of various appearances, all the films formed were α phase of fcc structure. In the process of the above-mentioned

TABLE I
List of Weight and Atomic Percentages of Hg for Ag–Hg Alloys[3]

Ag–Hg alloy phase	Hg content at room temperature	
	wt %	at %
α	0–50	0–36.5
β	60–61	44–45
γ	70–71	55.5–57

* Present address: Central Research Laboratories, Kuraray Co., Ltd., Kurashiki 710, Japan.

Journal of Applied Polymer Science, Vol. 29, 3813–3823 (1984)
© 1984 John Wiley & Sons, Inc. CCC 0021-8995/84/123813-11$04.00

investigation, however, we found that the remaining phases, β and γ, which are of hexagonal and bcc structure, respectively, can be produced by dropping Hg metal on the wet α-phase Ag–Hg alloy films formed on the surface of cast PAAm–$AgNO_3$ aqueous solution.

The purpose of this article is to establish the method of producing the β and γ phase Ag–Hg alloy films on polymer substrates by using PAAm–$AgNO_3$ aqueous solution and to identify the phases by X-ray analysis. Moreover, the lattice constants of the α-phase Ag–Hg alloy films are also studied in detail by an X-ray diffractometer to clarify their dependence on pH of the starting aqueous PAAm–$AgNO_3$ solution. Since the α phase is realized in a wide range of atomic ratio between Ag and Hg as shown in Table I, our films of different appearances may be attributed to different compositions.

pH DEPENDENCE OF LATTICE CONSTANT OF α PHASE

Sample Preparation

The α-phase Ag–Hg alloy films were prepared from the aqueous solution of 5 wt % PAAm (Sumitex Resin A-1, Sumitomo Chemical Industry Co. Ltd.) with $AgNO_3$ as described previously.[2] The molar concentration of Ag^+ to that of monomeric unit of PAAm, $F_1 = [Ag^+]/[MU]$, was fixed as 0.1 in the present study. In our previous paper,[2] we reported that the PAAm aqueous solution of different pH gives rise to different types of films: conductive whitish gray films from the solution of low pH and insulator films of metallic luster from the solution of high pH. Therefore, we prepared the following two series of the pH controlled solution:

(1) **Mixed Solution of Unrefined and Refined PAAm.** As stated in the previous paper,[2] pH of the 5 wt % aqueous solution of PAAm decreases from about 8.2 to 4.5 by refining PAAm in mixed solution of methanol and toluene with the mixing ratio of 3:1. Therefore, the pH can be controlled by mixing the unrefined and the refined PAAm solution.

(2) **Refined PAAm Solution with Ammonia.** As reported previously,[2] ammonia mainly determines pH of the aqueous solution of the unrefined PAAm; the existence of ammonia was recognized in the mixed solution of methanol and toluene used for refining. Therefore, the pH can be controlled by adding ammonia to the refined PAAm solution.

The existence of ammonia was also confirmed from the following pH change in the two series of starting solutions. Figures 1(a) and (b) show the pH changes by adding $AgNO_3$ up to the amount of $F_1 = 0.1$ to the solution of series 1 and the solution of series 2, respectively. The abscissa in each figure is taken as the mixing ratio of refined to unrefined PAAm or as the amount of ammonia added. The pH change may be attributed to the dissociation of protons due to the following reaction:

$$Ag^+ + 2NH_4^+ \rightarrow Ag(NH_3)_2^+ + 2H^+$$

The tendency of the pH change is quite similar to each other and confirms that ammonia plays a main part in determining the pH of the solution.

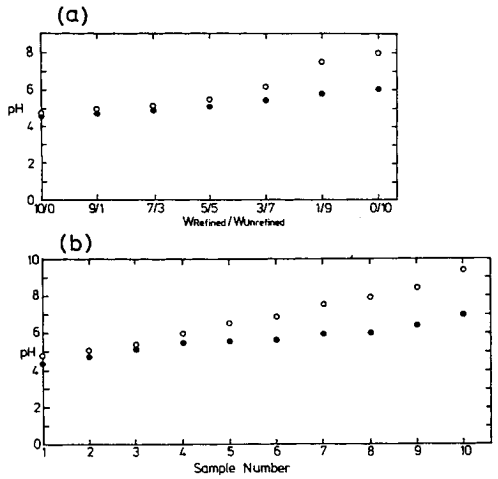

Fig. 1. Changes in pH of PAAm solution, observed when adding $AgNO_3$ up to the amount of $F_1 = 0.1$: (a) series 1, refined PAAm + unrefined PAAm; (b) series 2, refined PAAm + ammonia. (○) Before and (●) after adding $AgNO_3$.

X-Ray Analysis

Figure 2 shows X-ray Debye–Scherrer rings for the substances scraped off from the films of series 1. These are the typical patterns of α-phase Ag–Hg alloy of fcc structure as mentioned in our previous paper.[2] Careful analysis of these patterns leads to different lattice constants listed in Table II; the lattice constant clearly depends on pH of the starting solution.

X-ray diffraction patterns were also measured with a diffractometer (Philips PW1011 X-Ray Powder Diffractometer). We did not scrape off the substances from the film; the sample was the film itself, and its size was about 5×5 mm^2. Figures 3(a) and (b) are the typical results for the films of series 1 and 2, respectively. The films of each series were produced simultaneously in the same condition. The diffraction peak positions scatter even among the results of the same film as shown, for example, in the patterns of pH = 5.21 in Figure 3(a). Sometimes the peaks broaden or rather split into two as seen, for example, in the pattern of pH = 6.81 in Figure 3(b). In spite of these scattering, broadening, and splitting, which must originate

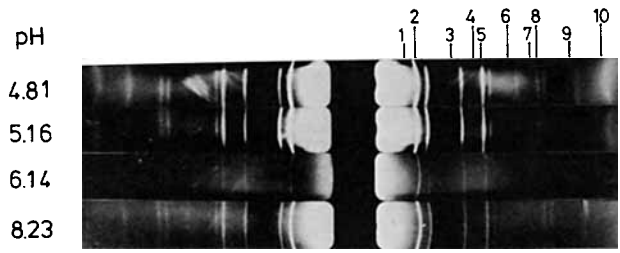

Fig. 2. X-ray Debye–Scherrer rings for the substances scraped off from the films formed by using pH controlled PAAm of series 1.

TABLE II
Lattice Constants Calculated from X-Ray Debye–Scherrer Rings for Films Formed by using pH-controlled PAAm of Series 1

pH	Lattice constants (Å)
4.81	4.141
5.16	4.131
6.14	4.085
8.23	4.080

from the lack of uniformity in the films produced, the tendency of shifting toward large angle side with increasing pH can clearly be seen.

The pH dependence of the scattering angle, i.e., the lattice constant a, is shown in Figure 4, where the results for series 1 and 2 are shown separately in (a) and (b), respectively. When there exist two peaks in the diffraction patterns, the results corresponding to the larger lattice constant are shown by closed circles and those corresponding to the smaller lattice constant by open circles. Paying attention only to the open circles, the dependence of the lattice constant on pH has the same tendency in both series. The lattice constant decreases with increasing pH; in other words, the Hg content in α phase decreases with increasing pH. The ordinate on right-hand side in Figures 4(a) or (b) shows Hg content estimated from the calibration curve

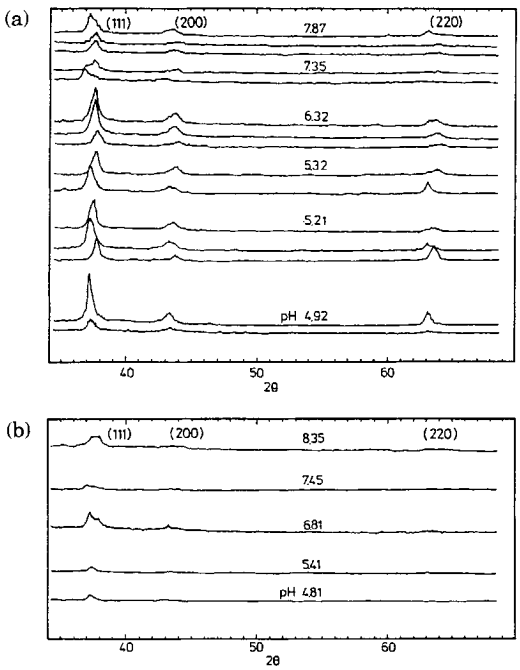

Fig. 3. X-ray diffraction peaks for the films formed by using pH controlled PAAm: (a) series 1, refined PAAm + unrefined PAAm; (b) series 2, refined PAAm + ammonia.

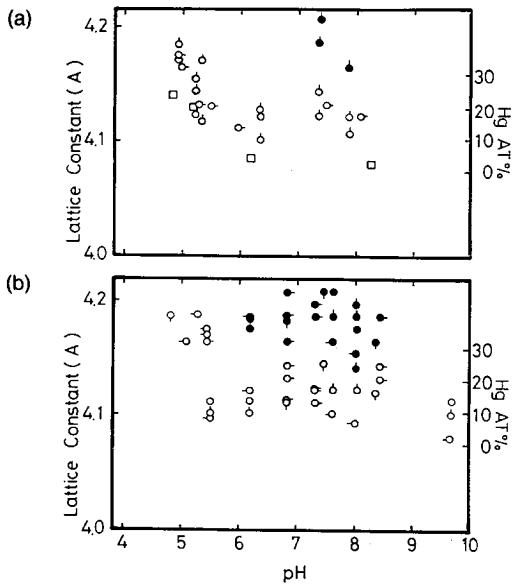

Fig. 4. pH dependence of lattice constants for the films formed by using pH controlled PAAm: (a) three experimental runs (⊖, ⏀ and □) for series 1; (⊘ and □) represent the data shown in Figures 3(a) and 2, respectively; (b) five experimental runs (○, ⏀, ⊖, ⚲ and ⊖) for series 2; (⚲ represents the data shown in Figure 3(b). For solid circles, See text.

given by Day and Mathewson.[4] In this way, the Hg content or the lattice constant is controllable by pH of the starting solution at least to some extent.

β- AND γ-PHASE Ag–Hg ALLOY FILMS

Sample Preparation

To increase the Hg concentration and to obtain Ag–Hg alloy films of β and/or γ phase shown in Table I, we tried to drop Hg metal in the following three ways:

1. After the casting of PAAm–$AgNO_3$ aqueous solution, but before the formation of α phase Ag–Hg alloy film.
2. After the film formation, but before its drying.
3. After the drying of the film.

When we drop Hg metal on the cast PAAm–$AgNO_3$ aqueous solution before the α-phase Ag–Hg alloy film is formed, the Hg metal sinks into the solution and causes the gelation of PAAm. Hence this method is not effective to produce the β- and/or γ-phase Ag–Hg alloy films. In the second way, Hg metal gradually diffuses on the surface if we leave it overnight at room temperature. The resulting film appears whitish and consists of the β and/or γ phase Ag–Hg alloy as shown in the next section. When we drop the Hg metal on the dried α-phase Ag–Hg alloy film, sometimes it diffuses but sometimes it does not, depending probably on the unknown surface condition. In this way, the only reliable method is the second one, and hence we adopt it in the following.

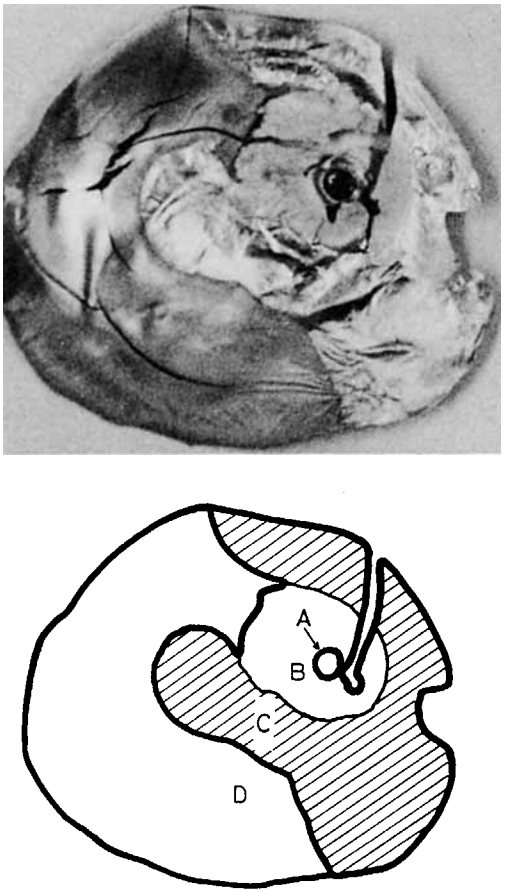

Fig. 5. Photograph and illustration for the diffusion of Hg. Hg metal is dropped at (A) and diffuses into (B) and (C) regions; it does not appear to reach (D) region.

X-Ray Analysis

Figure 5 illustrates a film thus produced. We can distinguish at least four regions, (A), (B), (C), and (D). From (A) region, where Hg metal is dropped, it diffuses into (B) region and then into (C) region, though it does not appear to reach (D) region. We scraped off the products from each region and tried to identify them by X-ray analysis. Figures 6–9 are the x-ray Debye-Scherrer rings for these products. Since region (C) is rather wide, we chose two places in the region: one, $(C)_B$, is close to (B) region and the other, $(C)_D$, is close to (D) region.

The product from (B) region appears to be identified as the γ-phase Ag–Hg alloy. The observed interplaner separations in Figure 6 for the product are listed in Table III and are compared with those of the γ-phase Ag–Hg alloy given in an ASTM card. The agreement in these line positions and their intensities is quite good except some weak lines which have no correspondence. The γ phase has the bcc structure with a lattice constant a = 10.013–10.031 Å,[5] while the present product gives a = 10.021 Å.

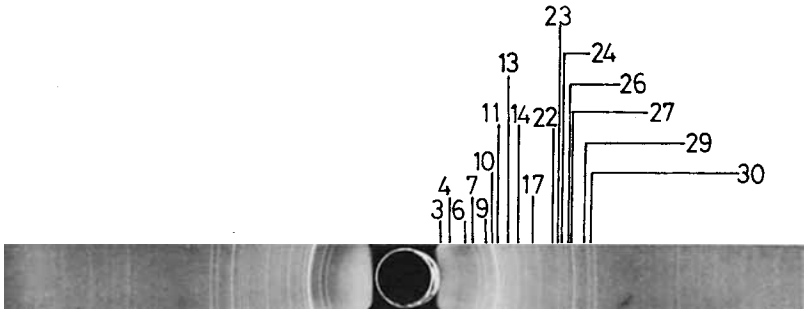

Fig. 6. X-ray Debye–Scherrer ring for (B) region.

TABLE III
Diffraction Intensity (Int) and Plane Distances (d) Observed by X-Ray Diffractometer for Film of (B) Region[a]

γ phase					
		Experiment		ASTM Card File 11-067	
Line	hkl	Int	d (Å)	I/I_1	d (Å)
1	110				
2	200				
3	211	W	4.114	10	4.080
4	220	W	3.548	10	3.530
5	310				
6	222	M	2.880	30	2.880
7	321	M	2.679	40	2.670
8	400				
9	411,330	S	2.365	100	2.360
10	420	MW	2.262	30	2.240
11	332	MW	2.134	30	2.130
12	422	W	2.040	10	2.050
13	510,431	M	1.965	40	1.965
14	521	MW	1.826	20	1.828
15	440				
16	530,433				
17	600,442	M	1.669	40	1.667
18	611,532	W	1.623	10	1.629
19	620			10	1.583
20	541	W	1.546	20	1.547
21	622			10	1.512
22	631	MW	1.479	30	1.478
23	444	MW	1.445	40	1.447
24	710,543	MW	1.416	40	1.419
25	640				
26	721,552	MS	1.362	70	1.365
27	642	W	1.339	20	1.341
28	730				
29	651,732	MW	1.269	50	1.275
30	811,741	M	1.231	60	1.236

[a] Those in ASTM Card File are shown for reference.

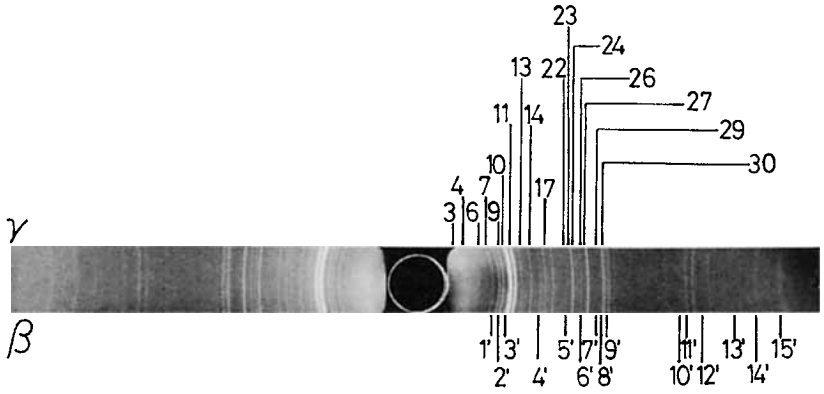

Fig. 7. X-ray Debye–Scherrer ring for $(C)_B$ region.

TABLE IV
Diffraction Intensity (Int) and Plane Distances (d) for Film of $(C)_B$ Region Observed by X-Ray Diffractometer[a]

γ phase					
		Experiment		ASTM Card File 11-067	
Line	*hkl*	Int	d (Å)	I/I_1	d (Å)
1	110				
2	200				
3	211	W	4.078	10	4.080
4	220	W	3.513	10	3.530
5	310				
6	222	M	2.871	30	2.880
7	321	M	2.663	40	2.670
8	400				
9	411,330	S	2.344	100	2.360
10	420	MS	2.254	30	2.240
11	332	MW	2.127	30	2.130
12	422			10	2.050
13	510,431	M	1.953	40	1.965
14	521	MW	1.817	20	1.828
15	440				
16	530,433				
17	600,442	M	1.663	40	1.667
18	611,532			10	1.629
19	620			10	1.583
20	541			20	1.547
21	622			10	1.512
22	631	M	1.475	30	1.478
23	444	MW	1.439	40	1.447
24	710,543	MW	1.411	40	1.419
25	640				
26	721,552	MS	1.358	70	1.365
27	642	W	1.335	20	1.341
28	730				
29	651,732	MW	1.261	50	1.275
30	811,741	M	1.234	60	1.236

TABLE IV (*continued from the previous page.*)

β phase					
		Experiment		ASTM Card File 27-618	
Line	*hkil*	Int	*d* (Å)	I/I_1	*d* (Å)
1′	$10\bar{1}0$	M	2.553	30	2.581
2′	0002	MS	2.392	50	2.420
3′	$10\bar{1}1$	S	2.254	100	2.273
4′	$10\bar{1}2$	MW	1.754	20	1.766
5′	$11\bar{2}0$	M	1.475	40	1.489
6′	$10\bar{1}3$	M	1.358	30	1.370
7′	$11\bar{2}2$	M	1.261	50	1.268
8′	$20\bar{2}1$	M	1.234	20	1.245
9′	0004	W	1.203	10	1.211
10′	$21\bar{3}1$	MW	0.950	50	0.954
11′	$11\bar{2}4$	MW	0.935	40	0.937
12′	$10\bar{1}5$	W	0.902	30	0.906
13′	$30\bar{3}0$	W	0.853	60	0.860
14′	$21\bar{3}3$	W	0.828	30	0.834
15′	$30\bar{3}2$	W	0.806	30	0.809

[a] Those in ASTM Card File are shown for reference.

The product from the $(C)_B$ region is a mixture of the γ and β phases as is clear in Figure 7 and Table IV, while the product from $(C)_D$ region is a mixture of the β and α phases, as shown in Figure 8 and Table V. The lattice constant of the γ phase in the product from $(C)_B$ is $a = 9.997$ Å, which agrees with the one from (B) region within an experimental error. The β-phase Ag–Hg alloy has the hexagonal structure with the lattice constant $a = 2.964$–2.987 Å and $c = 4.831 \sim 4.830$ Å.[5] The lattice constants determined from the present data are $a = 2.962$ Å and $c = 4.822$ Å for the product from $(C)_B$ and $a = 2.965$ Å and $c = 4.825$ Å from the product $(C)_D$: The agreement is satisfactory.

The product from the (D) region is expected to be the α phase; actually this is the case as shown in Figure 9 and Table VI. It is surprising that the α phase changes into the β and γ phases just by dropping Hg metal on the wet α-phase film surface. PAAm and/or its Ag chelate must play a significant role; the investigation to clarify the role is very interesting and is left as a future problem.

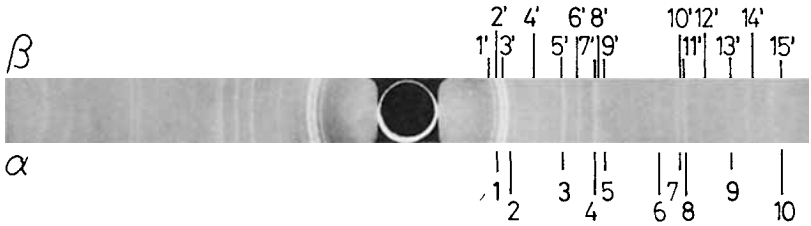

Fig. 8. X-ray Debye–Scherrer ring for $(C)_D$ region.

TABLE V
Diffraction Intensity (Int) and Plane Distances (d) for Film of $(C)_D$ Region[a]

β phase					
		Experiment		ASTM Card File 27-618	
Line	$hkil$	Int	d (Å)	I/I_1	d (Å)
1′	$10\bar{1}0$	M	2.553	30	2.581
2′	0002	MS	2.404	50	2.420
3′	$10\bar{1}1$	S	2.265	100	2.273
4′	$10\bar{1}2$	W	1.759	20	1.766
5′	$11\bar{2}0$	M	1.477	40	1.489
6′	$10\bar{1}3$	MW	1.362	30	1.370
7′	$11\bar{2}2$	M	1.261	50	1.268
8′	$20\bar{2}1$	MW	1.238	20	1.245
9′	0004	W	1.207	10	1.211
10′	$21\bar{3}1$	MW	0.952	50	0.954
11′	$11\bar{2}4$	MW	0.936	40	0.937
12′	$10\bar{1}5$	W	0.904	30	0.906
13′	$30\bar{3}0$	W	0.854	60	0.860
14′	$21\bar{3}3$	W	0.831	30	0.834
15′	$30\bar{3}2$	W	0.807	30	0.809

α phase					
		Experiment		Pure Ag experiment	
Line	hkl	Int	d (Å)	Int	d (Å)
1	111	S	2.368	S	2.350
2	200	W	2.101	MW	2.027
3	220	M	1.477	MS	1.437
4	311	MW	1.238	MS	1.226
5	222	W	1.207	MW	1.173
6	400	W	1.004	W	1.019
7	331	MW	0.952	M	0.935
8	420	MW	0.936	M	0.913
9	422	W	0.854	M	0.833
10	333,511	W	0.807	M	0.786

[a] Those in ASTM Card File and experimental results for pure Ag are shown for reference.

Fig. 9. X-ray Debye–Scherrer ring for (D) region.

TABLE VI
Diffraction Intensity (Int) and Plane Distances (d) for Film of (D) Region[a]

α phase					
		Experiment		Pure Ag experiment	
Line	*hkl*	Int	d (Å)	Int	d (Å)
1	111	S	2.368	S	2.350
2	200	M	2.058	MW	2.027
3	220	M	1.452	MS	1.437
4	311	M	1.238	MS	1.226
5	222	MW	1.186	MW	1.173
6	400			W	1.019
7	331	MW	0.939	M	0.935
8	420	MW	0.920	M	0.913
9	422	W	0.839	M	0.833
10	333,511	W	0.790	M	0.786

[a] Experimental results for pure Ag are shown for reference.

We wish to thank Dr. O. Sumita in Hitachi Engineering Co. for his help in the early stage of the present study.

References

1. T. Chitani, *Inorganic Chemistry (I)*, Sangyo Tosho, Tokyo, 1963, p. 162 (in Japanese).
2. J. Y. Lee, H. Tanaka, H. Takezoe, A. Fukuda, E. Kuze, and H. Iwanaga, *J. Appl. Polym. Sci.*, **29**, 795 (1984).
3. A. J. Murphy, *J. Inst. Metals*, **46**, 507 (1931).
4. H. M. Day and C. H. Mathewson, *Trans. Am. Inst. Mining Metall. Eng.*, **128**, 261 (1938).
5. W. B. Pearson, *A Handbook of Lattice Spacing and Structures of Metals and Alloys*, Pergamon Press, Oxford, 1958, p. 285.

Received February 29, 1984
Accepted March 20, 1984